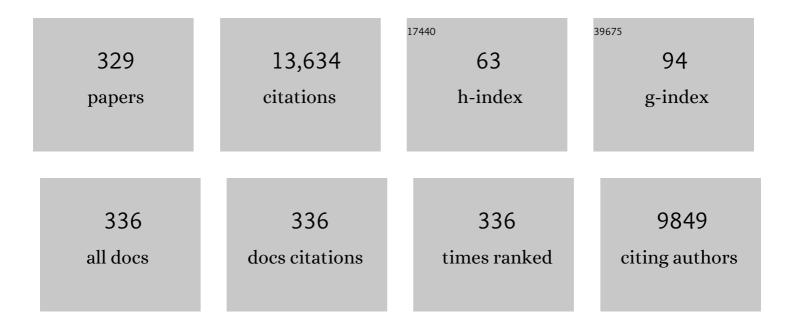
Yao-Yu Wang

List of Publications by Year in descending order

Source: https://exaly.com/author-pdf/2045035/publications.pdf Version: 2024-02-01



#	Article	IF	CITATIONS
1	Uncommon Pyrazoyl-Carboxyl Bifunctional Ligand-Based Microporous Lanthanide Systems: Sorption and Luminescent Sensing Properties. Inorganic Chemistry, 2016, 55, 3952-3959.	4.0	276
2	Preparation and Post-Assembly Modification of Metallosupramolecular Assemblies from Poly(<i>N</i> -Heterocyclic Carbene) Ligands. Chemical Reviews, 2018, 118, 9587-9641.	47.7	254
3	Four uncommon nanocage-based Ln-MOFs: highly selective luminescent sensing for Cu ²⁺ ions and selective CO ₂ capture. Chemical Communications, 2014, 50, 8731.	4.1	245
4	Copper-Catalyzed Coupling of Oxime Acetates with Aldehydes: A New Strategy for Synthesis of Pyridines. Organic Letters, 2011, 13, 5394-5397.	4.6	220
5	Three new solvent-directed Cd(<scp>ii</scp>)-based MOFs with unique luminescent properties and highly selective sensors for Cu ²⁺ cations and nitrobenzene. Dalton Transactions, 2015, 44, 3271-3277.	3.3	203
6	Textiles/Metal–Organic Frameworks Composites as Flexible Air Filters for Efficient Particulate Matter Removal. ACS Applied Materials & Interfaces, 2019, 11, 17368-17374.	8.0	175
7	Porous MOF with Highly Efficient Selectivity and Chemical Conversion for CO ₂ . ACS Applied Materials & Interfaces, 2017, 9, 17969-17976.	8.0	173
8	Molecular braids in metal–organic frameworks. Chemical Society Reviews, 2012, 41, 6992.	38.1	166
9	Four super water-stable lanthanide–organic frameworks with active uncoordinated carboxylic and pyridyl groups for selective luminescence sensing of Fe ³⁺ . Dalton Transactions, 2015, 44, 13325-13330.	3.3	164
10	A robust cluster-based Eu-MOF as multi-functional fluorescence sensor for detection of antibiotics and pesticides in water. Sensors and Actuators B: Chemical, 2021, 331, 129377.	7.8	155
11	Ruthenium-Catalyzed Cyclization of Ketoxime Acetates with DMF for Synthesis of Symmetrical Pyridines. Organic Letters, 2014, 16, 3082-3085.	4.6	153
12	A rod packing microporous metal–organic framework: unprecedented <i>ukv</i> topology, high sorption selectivity and affinity for CO ₂ . Chemical Communications, 2011, 47, 5464-5466.	4.1	152
13	InÂVitro Expansion of Primary Human Hepatocytes with Efficient Liver Repopulation Capacity. Cell Stem Cell, 2018, 23, 806-819.e4.	11.1	145
14	Two 3D Isostructural Ln(III)-MOFs: Displaying the Slow Magnetic Relaxation and Luminescence Properties in Detection of Nitrobenzene and Cr ₂ O ₇ ^{2–} . Inorganic Chemistry, 2016, 55, 11323-11330.	4.0	142
15	Supramolecular control of MOF pore properties for the tailored guest adsorption/separation applications. Coordination Chemistry Reviews, 2021, 434, 213709.	18.8	141
16	Honeycomb Metal–Organic Framework with Lewis Acidic and Basic Bifunctional Sites: Selective Adsorption and CO ₂ Catalytic Fixation. ACS Applied Materials & Interfaces, 2018, 10, 10965-10973.	8.0	138
17	Three new luminescent Cd(<scp>ii</scp>)-MOFs by regulating the tetracarboxylate and auxiliary co-ligands, displaying high sensitivity for Fe ³⁺ in aqueous solution. Dalton Transactions, 2015, 44, 10385-10391.	3.3	132
18	Multifunctional Coating Based on Hyaluronic Acid and Dopamine Conjugate for Potential Application on Surface Modification of Cardiovascular Implanted Devices. ACS Applied Materials & Interfaces, 2016, 8, 109-121.	8.0	132

#	Article	IF	CITATIONS
19	Investigation on the prime factors influencing the formation of entangled metal–organic frameworks. CrystEngComm, 2013, 15, 2561.	2.6	131
20	Immobilization of heparin/poly-l-lysine nanoparticles on dopamine-coated surface to create a heparin density gradient for selective direction of platelet and vascular cells behavior. Acta Biomaterialia, 2014, 10, 1940-1954.	8.3	126
21	Multifunctional Textiles/Metalâ~'Organic Frameworks Composites for Efficient Ultraviolet Radiation Blocking and Noise Reduction. ACS Applied Materials & Interfaces, 2020, 12, 55316-55323.	8.0	124
22	Efficient light hydrocarbon separation and CO ₂ capture and conversion in a stable MOF with oxalamide-decorated polar tubes. Chemical Communications, 2017, 53, 12970-12973.	4.1	121
23	Palladium atalyzed Oxidative Carbonylation of the Alkenyl Cï£;H Bonds of Enamides: Synthesis of 1,3â€Oxazinâ€6â€ones. Angewandte Chemie - International Edition, 2013, 52, 14196-14199.	13.8	120
24	Highly selective luminescence sensing for the detection of nitrobenzene and Fe ³⁺ by new Cd(<scp>ii</scp>)-based MOFs. CrystEngComm, 2018, 20, 477-486.	2.6	119
25	Iron-Catalyzed Cyclization of Ketoxime Carboxylates and Tertiary Anilines for the Synthesis of Pyridines. Organic Letters, 2016, 18, 1194-1197.	4.6	118
26	A first new porous d–p HMOF material with multiple active sites for excellent CO ₂ capture and catalysis. Chemical Communications, 2020, 56, 2395-2398.	4.1	116
27	Two porous luminescent metal–organic frameworks: quantifiable evaluation of dynamic and static luminescent sensing mechanisms towards Fe ³⁺ . Dalton Transactions, 2015, 44, 17222-17228.	3.3	114
28	An Uncommon Carboxylâ€Decorated Metal–Organic Framework with Selective Gas Adsorption and Catalytic Conversion of CO ₂ . Chemistry - A European Journal, 2018, 24, 865-871.	3.3	112
29	Rapid Assembly of Diversely Functionalized Spiroindenes by a Threeâ€Component Palladiumâ€Catalyzed Câ [°] 'H Amination/Phenol Dearomatization Domino Reaction. Angewandte Chemie - International Edition, 2017, 56, 14257-14261.	13.8	109
30	Thiol-Functionalized Pores via Post-Synthesis Modification in a Metal–Organic Framework with Selective Removal of Hg(II) in Water. Inorganic Chemistry, 2019, 58, 3409-3415.	4.0	109
31	Highly Waterâ€&table Lanthanide–Oxalate MOFs with Remarkable Proton Conductivity and Tunable Luminescence. Advanced Materials, 2017, 29, 1701804.	21.0	106
32	Copper-catalyzed homocoupling of ketoxime carboxylates for synthesis of symmetrical pyrroles. Green Chemistry, 2014, 16, 112-115.	9.0	104
33	Novel cage-like MOF for gas separation, CO ₂ conversion and selective adsorption of an organic dye. Inorganic Chemistry Frontiers, 2020, 7, 746-755.	6.0	99
34	Highly Stereoselective Synthesis of Imineâ€Containing Dibenzo[<i>b</i> , <i>d</i>]azepines by a Palladium(II)â€Catalyzed [5+2] Oxidative Annulation of <i>o</i> â€Arylanilines with Alkynes. Angewandte Chemie - International Edition, 2015, 54, 15385-15389.	13.8	98
35	Four new metal–organic frameworks based on diverse secondary building units: sensing and magnetic properties. Dalton Transactions, 2018, 47, 1682-1692.	3.3	98
36	Five sra Topological Ln(III)-MOFs Based on Novel Metal-Carboxylate/Cl Chain: Structure, Near-Infrared Luminescence and Magnetic Properties. Crystal Growth and Design, 2013, 13, 1570-1576.	3.0	95

#	Article	IF	CITATIONS
37	Ultrastable and Highly Catalytically Active Nâ€Heterocyclicâ€Carbeneâ€Stabilized Gold Nanoparticles in Confined Spaces. Angewandte Chemie - International Édition, 2020, 59, 16683-16689.	13.8	92
38	Strategy for the Construction of Diverse Polyâ€NHCâ€Derived Assemblies and Their Photoinduced Transformations. Angewandte Chemie - International Edition, 2020, 59, 10073-10080.	13.8	89
39	Thermoelectric properties of PEDOT nanowire/PEDOT hybrids. Nanoscale, 2016, 8, 8033-8041.	5.6	88
40	A microporous anionic metal–organic framework for a highly selective and sensitive electrochemical sensor of Cu ²⁺ ions. Chemical Communications, 2016, 52, 8475-8478.	4.1	88
41	Tetrahedral Anion Cage: Selfâ€Assembly of a (PO ₄) ₄ L ₄ Complex from a Tris(bisurea) Ligand. Angewandte Chemie - International Edition, 2013, 52, 5096-5100.	13.8	87
42	Homo―and Heteroligand Polyâ€NHC Metal Assemblies: Synthesis by Narcissistic and Social Selfâ€&orting. Angewandte Chemie - International Edition, 2018, 57, 15767-15771.	13.8	87
43	Self-Assembly, Structural Transformation, and Guest-Binding Properties of Supramolecular Assemblies with Triangular Metal–Metal Bonded Units. Journal of the American Chemical Society, 2020, 142, 2524-2531.	13.7	84
44	Controlling Molecular Weight of Hyaluronic Acid Conjugated on Amine-rich Surface: Toward Better Multifunctional Biomaterials for Cardiovascular Implants. ACS Applied Materials & Interfaces, 2017, 9, 30343-30358.	8.0	83
45	Supramolecular Control of Photocycloadditions in Solution: In Situ Stereoselective Synthesis and Release of Cyclobutanes. Angewandte Chemie - International Edition, 2019, 58, 3986-3991.	13.8	83
46	Luminescence Modulation, White Light Emission, and Energy Transfer in a Family of Lanthanide Metal–Organic Frameworks Based on a Planar ï€-Conjugated Ligand. Crystal Growth and Design, 2017, 17, 4217-4224.	3.0	82
47	Encapsulation of Halocarbons in a Tetrahedral Anion Cage. Angewandte Chemie - International Edition, 2015, 54, 8658-8661.	13.8	81
48	Air- and Light-Stable P ₄ and As ₄ within an Anion-Coordination-Based Tetrahedral Cage. Journal of the American Chemical Society, 2017, 139, 5946-5951.	13.7	80
49	Palladium atalyzed Carbonylation of Amines: Switchable Approaches to Carbamates and <i>N,N′</i> â€Disubstituted Ureas. Advanced Synthesis and Catalysis, 2012, 354, 489-496.	4.3	78
50	Hierarchically porous sheath–core graphene-based fiber-shaped supercapacitors with high energy density. Journal of Materials Chemistry A, 2018, 6, 896-907.	10.3	77
51	Peripheral Templationâ€Modulated Interconversion between an A ₄ L ₆ Tetrahedral Anion Cage and A ₂ L ₃ Triple Helicate with Guest Capture/Release. Angewandte Chemie - International Edition, 2018, 57, 1851-1855.	13.8	76
52	A Strategy for the Construction of Triply Interlocked Organometallic Cages by Rational Design of Poly-NHC Precursors. Journal of the American Chemical Society, 2020, 142, 13614-13621.	13.7	74
53	Recent progresses in luminescent metal–organic frameworks (LMOFs) as sensors for the detection of anions and cations in aqueous solution. Dalton Transactions, 2021, 50, 1950-1972.	3.3	74
54	Copper-catalyzed 5-endo-trig cyclization of ketoxime carboxylates: a facile synthesis of 2-arylpyrroles. Chemical Communications, 2014, 50, 7437.	4.1	73

#	Article	IF	CITATIONS
55	Synthesis of Enamides via Cul-Catalyzed Reductive Acylation of Ketoximes with NaHSO3. Journal of Organic Chemistry, 2011, 76, 339-341.	3.2	72
56	A Cationic MOF with High Uptake and Selectivity for CO ₂ due to Multiple CO ₂ â€Philic Sites. Chemistry - A European Journal, 2015, 21, 16525-16531.	3.3	72
57	A New Porous MOF with Two Uncommon Metal–Carboxylate–Pyrazolate Clusters and High CO ₂ /N ₂ Selectivity. Inorganic Chemistry, 2015, 54, 1841-1846.	4.0	71
58	Solvent-free method to encapsulate polyoxometalate into metal-organic frameworks as efficient and recyclable photocatalyst for harmful sulfamethazine degrading in water. Applied Catalysis B: Environmental, 2019, 245, 753-759.	20.2	70
59	Structural diversity of five new bitriazole-based complexes: luminescence, sorption, and magnetic properties. Dalton Transactions, 2015, 44, 1110-1119.	3.3	69
60	Multiple Functions of Gas Separation and Vapor Adsorption in a New MOF with Open Tubular Channels. ACS Applied Materials & Interfaces, 2021, 13, 4102-4109.	8.0	67
61	Solvents influence on sizes of channels in three fry topological Mn(ii)-MOFs based on metal–carboxylate chains: syntheses, structures and magnetic properties. CrystEngComm, 2013, 15, 8125.	2.6	66
62	A new stable luminescent Cd(<scp>ii</scp>) metal–organic framework with fluorescent sensing and selective dye adsorption properties. Dalton Transactions, 2018, 47, 9466-9473.	3.3	65
63	Coupling of enamides with alkynes or arynes for synthesis of substituted pyridines and isoquinolines via amide activation. Chemical Communications, 2012, 48, 8105.	4.1	64
64	Highly selective luminescence sensing for Cu ²⁺ ions and selective CO ₂ capture in a doubly interpenetrated MOF with Lewis basic pyridyl sites. Dalton Transactions, 2015, 44, 4423-4427.	3.3	64
65	Efficient C ₂ H <i>_n</i> Hydrocarbons and VOC Adsorption and Separation in an MOF with Lewis Basic and Acidic Decorated Active Sites. ACS Applied Materials & Interfaces, 2020, 12, 41785-41793.	8.0	64
66	Template-Directed Photochemical [2 + 2] Cycloaddition in Crystalline Materials: A Useful Tool to Access Cyclobutane Derivatives. Crystal Growth and Design, 2018, 18, 553-565.	3.0	63
67	Supramolecular Control of Photocycloadditions in Solution: In Situ Stereoselective Synthesis and Release of Cyclobutanes. Angewandte Chemie, 2019, 131, 4026-4031.	2.0	63
68	Two Series of Microporous Lanthanide–Organic Frameworks with Different Secondary Building Units and Exposed Lewis Base Active Sites: Sensing, Dye Adsorption, and Magnetic Properties. Inorganic Chemistry, 2019, 58, 339-348.	4.0	63
69	Tuning the Magnetic Interactions in Dy(III) ₄ Single-Molecule Magnets. Inorganic Chemistry, 2018, 57, 8550-8557.	4.0	62
70	Synthesis of symmetrical pyridines by iron-catalyzed cyclization of ketoxime acetates and aldehydes. Green Chemistry, 2017, 19, 1023-1027.	9.0	61
71	Photodynamic antimicrobial chemotherapy for Staphylococcus aureus and multidrug-resistant bacterial burn infection in vitro and in vivo. International Journal of Nanomedicine, 2017, Volume 12, 5915-5931.	6.7	61
72	Palladium-Catalyzed Carbonylation of Indoles for Synthesis of Indol-3-yl Aryl Ketones. ACS Catalysis, 2015, 5, 1210-1213.	11.2	60

#	Article	IF	CITATIONS
73	Creation of Sub-diffraction Longitudinally Polarized Spot by Focusing Radially Polarized Light with Binary Phase Lens. Scientific Reports, 2016, 6, 38859.	3.3	60
74	Oxide-based RRAM: Unified microscopic principle for both unipolar and bipolar switching. , 2011, , .		58
75	Dynamic Zn-based metal–organic framework: stepwise adsorption, hysteretic desorption and selective carbon dioxide uptake. Journal of Materials Chemistry A, 2013, 1, 6535.	10.3	58
76	Solvent Influence on Sizes of Channels in Three New Co(II) Complexes, Exhibiting an Active Replaceable Coordinated Site. Crystal Growth and Design, 2013, 13, 66-73.	3.0	57
77	Three new solvent-directed 3D lead(ii)–MOFs displaying the unique properties of luminescence and selective CO2 sorption. Dalton Transactions, 2013, 42, 13590.	3.3	57
78	Tunable Emission and Selective Luminescence Sensing in a Series of Lanthanide Metal–Organic Frameworks with Uncoordinated Lewis Basic Triazolyl Sites. Crystal Growth and Design, 2018, 18, 2031-2039.	3.0	57
79	One‣tep C ₂ H ₄ Purification from Ternary C ₂ H ₆ /C ₂ H _{/C₂H₂Mixtures by a Robust Metal–Organic Framework with Customized Pore Environment. Angewandte Chemie - International Edition. 2022. 61}	13.8	57
80	A Rare L1D + R1D → 3D Luminescent Dense Polymer as Multifunctional Sensor to Nitro Aromatic Compounds, Cu ²⁺ , and Bases. Crystal Growth and Design, 2014, 14, 2954-2961.	3.0	56
81	Copperâ€Catalyzed Direct Synthesis of Iodoenamides from Ketoximes. Chemistry - A European Journal, 2013, 19, 9789-9794.	3.3	55
82	Series of Water-Stable Lanthanide Metal–Organic Frameworks Based on Carboxylic Acid Imidazolium Chloride: Tunable Luminescent Emission and Sensing. Inorganic Chemistry, 2019, 58, 13969-13978.	4.0	55
83	Facile Incorporation of Au Nanoparticles into an Unusual Twofold Entangled Zn(II)-MOF with Nanocages for Highly Efficient CO ₂ Fixation under Mild Conditions. ACS Applied Materials & Interfaces, 2019, 11, 47437-47445.	8.0	55
84	Syntheses and Crystal Structures of a Series of Zn(II)/Cd(II) Coordination Polymers Constructed from a Flexible 6,6′-Dithiodinicotinic Acid. Crystal Growth and Design, 2011, 11, 1531-1541.	3.0	53
85	Stable Indium-Pyridylcarboxylate Framework: Selective Gas Capture and Sensing of Fe ³⁺ Ion in Water. Inorganic Chemistry, 2018, 57, 15262-15269.	4.0	53
86	C ₃ ‣ymmetric Assemblies from Trigonal Polycarbene Ligands and M ^I Ions for the Synthesis of Threeâ€Dimensional Polyimidazolium Cations. Angewandte Chemie - International Edition, 2019, 58, 13360-13364.	13.8	53
87	A novel coating of type IV collagen and hyaluronic acid on stent material-titanium for promoting smooth muscle cell contractile phenotype. Materials Science and Engineering C, 2014, 38, 235-243.	7.3	52
88	New Doubly Interpenetrated MOF with [Zn ₄ 0] Clusters and Its Doped Isomorphic MOF: Sensing, Dye, and Gas Adsorption Capacity. Crystal Growth and Design, 2019, 19, 6774-6783.	3.0	52
89	Highly stable 3D porous HMOF with enhanced catalysis and fine color regulation by the combination of d- and p-ions when compared with those of its monometallic MOFs. Chemical Communications, 2020, 56, 8758-8761.	4.1	52
90	Two comparable Ba-MOFs with similar linkers for enhanced CO2 capture and separation by introducing N-rich groups. Rare Metals, 2021, 40, 499-504.	7.1	52

#	Article	IF	CITATIONS
91	Microwave versus Traditional Solvothermal Synthesis of Ni ₇ ^{II} Discs: Effect of Ligand on Exchange Reaction in Solution Studied by Electrospray Ionization-Mass Spectroscopy and Magnetic Properties. Inorganic Chemistry, 2011, 50, 7274-7283.	4.0	51
92	High CO ₂ Uptake Capacity and Selectivity in a Fascinating Nanotube-Based Metal–Organic Framework. Inorganic Chemistry, 2017, 56, 908-913.	4.0	51
93	Nonenzymatic Glucose Sensing and Magnetic Property Based On the Composite Formed by Encapsulating Ag Nanoparticles in Cluster-Based Co-MOF. Inorganic Chemistry, 2019, 58, 16743-16751.	4.0	51
94	Two Stable Terbium–Organic Frameworks Based on Predesigned Functionalized Ligands: Selective Sensing of Fe3+ Ions and C2H2/CH4 Separation. Inorganic Chemistry, 2019, 58, 10295-10303.	4.0	50
95	Effect of Coordinated Solvent Molecules on Metal Coordination Sphere and Solvent-Induced Transformations. Crystal Growth and Design, 2017, 17, 517-526.	3.0	49
96	Rational construction of a stable Zn ₄ O-based MOF for highly efficient CO ₂ capture and conversion. Chemical Communications, 2018, 54, 456-459.	4.1	48
97	Thermoelectric Properties of Conducting Polymer Nanowire–Tellurium Nanowire Composites. ACS Applied Energy Materials, 2018, 1, 4883-4890.	5.1	48
98	Transitions of two magnetic interaction states in dinuclear Dy(<scp>iii</scp>) complexes via subtle structural variations. Dalton Transactions, 2017, 46, 638-642.	3.3	47
99	MOF-COF Composite Photocatalysts: Design, Synthesis, and Mechanism. Crystal Growth and Design, 2022, 22, 893-908.	3.0	47
100	Two Isostructural Metal–Organic Frameworks Directed by the Different Center Metal Ions, Exhibiting the Ferrimagnetic Behavior and Slow Magnetic Relaxation. Inorganic Chemistry, 2016, 55, 6592-6596.	4.0	45
101	Uptake and transformation of steroid estrogens as emerging contaminants influence plant development. Environmental Pollution, 2018, 243, 1487-1497.	7.5	45
102	Backboneâ€Directed Selfâ€Assembly of Interlocked Molecular Cyclic Metalla[3]Catenanes. Angewandte Chemie - International Edition, 2020, 59, 13516-13520.	13.8	45
103	Recent advances of functional heterometallic-organic framework (HMOF) materials: Design strategies and applications. Coordination Chemistry Reviews, 2022, 463, 214521.	18.8	45
104	Positional isomeric tunable two Co(<scp>ii</scp>) 6-connected 3-D frameworks with pentanuclear to binuclear units: structures, ion-exchange and magnetic properties. Dalton Transactions, 2014, 43, 15450-15456.	3.3	44
105	Series of Cd(II) and Pb(II) Coordination Polymers Based on a Multilinker (<i>R,S</i> -)2,2′-Bipyridine-3,3′-dicarboxylate-1,1′-dioxide. Crystal Growth and Design, 2014, 14, 5466-5	4 ³ 6 ⁰	43
106	Tailoring of the titanium surface by preparing cardiovascular endothelial extracellular matrix layer on the hyaluronic acid micro-pattern for improving biocompatibility. Colloids and Surfaces B: Biointerfaces, 2015, 128, 201-210.	5.0	43
107	Structural Diversity of Cadmium(II) Coordination Polymers Induced by Tuning the Coordination Sites of Isomeric Ligands. Inorganic Chemistry, 2016, 55, 8871-8880.	4.0	43
108	Temperature-Induced Syntheses, Iodine Elimination, Enantiomers Resolution, and Single-Crystal-to-Single-Crystal Transformation of Imidazole-Co(II) Coordination Polymers with Amino-isophthalic Acid as Co-Ligand. Crystal Growth and Design, 2016, 16, 3961-3968.	3.0	43

#	Article	IF	CITATIONS
109	Post-Synthetic Functionalization of Ni-MOF by Eu ³⁺ Ions: Luminescent Probe for Aspartic Acid and Magnetic Property. Inorganic Chemistry, 2020, 59, 7531-7538.	4.0	43
110	New multifunctional 3D porous metal–organic framework with selective gas adsorption, efficient chemical fixation of CO ₂ and dye adsorption. Dalton Transactions, 2019, 48, 7612-7618.	3.3	41
111	Fine-tuning terminal solvent ligands to rationally enhance the energy barrier in dinuclear dysprosium single-molecule magnets. Dalton Transactions, 2017, 46, 186-192.	3.3	40
112	Peripheral Templationâ€Modulated Interconversion between an A ₄ L ₆ Tetrahedral Anion Cage and A ₂ L ₃ Triple Helicate with Guest Capture/Release. Angewandte Chemie, 2018, 130, 1869-1873.	2.0	40
113	A highly stable MOF with F and N accessible sites for efficient capture and separation of acetylene from ternary mixtures. Journal of Materials Chemistry A, 2021, 9, 24495-24502.	10.3	40
114	The endothelialization and hemocompatibility of the functional multilayer on titanium surface constructed with type IV collagen and heparin. Colloids and Surfaces B: Biointerfaces, 2013, 108, 295-304.	5.0	39
115	Super-oscillatory focusing of circularly polarized light by ultra-long focal length planar lens based on binary amplitude-phase modulation. Scientific Reports, 2016, 6, 29068.	3.3	39
116	Synthesis of tetrasubstituted symmetrical pyridines by iron-catalyzed cyclization of ketoxime acetates. Organic Chemistry Frontiers, 2017, 4, 597-602.	4.5	39
117	New Luminescent Three-Dimensional Zn(II)/Cd(II)-Based Metal–Organic Frameworks Showing High H ₂ Uptake and CO ₂ Selectivity Capacity. Crystal Growth and Design, 2017, 17, 2059-2065.	3.0	39
118	Seven luminescent metal–organic frameworks constructed from 5-(triazol-1-yl)nicotinic acid: luminescent sensors for Cr ^{VI} and MnO ₄ ^{â^'} ions in an aqueous medium. New Journal of Chemistry, 2018, 42, 9865-9875.	2.8	39
119	A new honeycomb metal–carboxylate-tetrazolate framework with multiple functions for CO ₂ conversion and selective capture of C ₂ H ₂ , CO ₂ and benzene. Inorganic Chemistry Frontiers, 2020, 7, 1957-1964.	6.0	39
120	Four new lanthanide–organic frameworks: selective luminescent sensing and magnetic properties. Dalton Transactions, 2016, 45, 12800-12806.	3.3	38
121	A Multi-Functional In(III)-Organic Framework for Acetylene Separation, Carbon Dioxide Utilization, and Antibiotic Detection in Water. Inorganic Chemistry, 2020, 59, 15302-15311.	4.0	38
122	Two Microporous Metal–Organic Frameworks with Suitable Pore Size Displaying the High CO ₂ /CH ₄ Selectivity. Crystal Growth and Design, 2015, 15, 5382-5387.	3.0	37
123	Bisphenol a electrochemical sensor based on multi-walled carbon nanotubes/polythiophene/Pt nanocomposites modified electrode. Analytical Methods, 2016, 8, 3333-3338.	2.7	37
124	Engineering Cardiovascular Implant Surfaces to Create a Vascular Endothelial Growth Microenvironment. Biotechnology Journal, 2017, 12, 1600401.	3.5	37
125	Four New 3D Metal–Organic Frameworks Constructed by a V-shaped Tetracarboxylates Ligand: Selective CO ₂ Sorption and Luminescent Sensing. Crystal Growth and Design, 2017, 17, 6733-6740.	3.0	37
126	Five New Cd(II) Complexes Induced by Reaction Conditions and Coordination Modes of 5-(1 <i>H</i> -Tetrazol-5-yl)isophthalic Acid Ligand: Structures and Luminescence. Crystal Growth and Design, 2016, 16, 5394-5402.	3.0	36

#	Article	IF	CITATIONS
127	Efficient gas and alcohol uptake and separation driven by two types of channels in a porous MOF: an experimental and theoretical investigation. Journal of Materials Chemistry A, 2020, 8, 5227-5233.	10.3	36
128	Syntheses of three new isostructural lanthanide coordination polymers with tunable emission colours through bimetallic doping, and their luminescence sensing properties. Dalton Transactions, 2019, 48, 13607-13613.	3.3	35
129	Luminescence modulation, near white light emission, selective luminescence sensing, and anticounterfeiting <i>via</i> a series of Ln-MOFs with a i€-conjugated and uncoordinated lewis basic triazolyl ligand. Inorganic Chemistry Frontiers, 2021, 8, 329-338.	6.0	35
130	Two new pH-controlled metal–organic frameworks based on polynuclear secondary building units with conformation-flexible cyclohexane-1,2,4,5-tetracarboxylate ligand. Inorganica Chimica Acta, 2011, 367, 127-134.	2.4	34
131	Two Nanocage-Based Metal–Organic Frameworks with Mixed-Cluster SBUs and CO2 Sorption Selectivity. Inorganic Chemistry, 2015, 54, 8937-8942.	4.0	34
132	Direct Evidence: Enhanced C ₂ H ₆ and C ₂ H ₄ Adsorption and Separation Performances by Introducing Open Nitrogen-Donor Sites in a MOF. Inorganic Chemistry, 2018, 57, 12417-12423.	4.0	34
133	Performance enhancement of oxygen evolution reaction through incorporating bimetallic electrocatalysts in two-dimensional metal–organic frameworks. Catalysis Science and Technology, 2020, 10, 3897-3903.	4.1	34
134	Design and Synthesis of Fluorescent Nanocelluloses for Sensing and Bioimaging Applications. ChemPlusChem, 2020, 85, 487-502.	2.8	34
135	Structural characterization and luminescence behavior of a 2D silver (I) coordination polymer assembled from pyridine-2,6-dicarboxylic acid N-oxide. Inorganic Chemistry Communication, 2006, 9, 645-648.	3.9	33
136	Controlling mesenchymal stem cells differentiate into contractile smooth muscle cells on a TiO2 micro/nano interface: Towards benign pericytes environment for endothelialization. Colloids and Surfaces B: Biointerfaces, 2016, 145, 410-419.	5.0	33
137	Functionalization of MOFs <i>via</i> a mixed-ligand strategy: enhanced CO ₂ uptake by pore surface modification. Dalton Transactions, 2018, 47, 5298-5303.	3.3	33
138	Five transition metal coordination polymers driven by a semirigid trifunctional nicotinic acid ligand: selective adsorption and magnetic properties. CrystEngComm, 2018, 20, 5726-5734.	2.6	33
139	Two isostructural amine-functionalized 3D self-penetrating microporous MOFs exhibiting high sorption selectivity for CO2. CrystEngComm, 2013, 15, 2057.	2.6	32
140	Efficient Asymmetric Biomimetic Aldol Reaction of Glycinates and Trifluoromethyl Ketones by Carbonyl Catalysis. Angewandte Chemie - International Edition, 2021, 60, 20166-20172.	13.8	32
141	Multiple fluorescence response behaviors towards antibiotics and bacteria based on a highly stable Cd-MOF. Journal of Hazardous Materials, 2022, 423, 127132.	12.4	32
142	Ultra-light-weight kevlar/polyimide 3D woven spacer multifunctional composites for high-gain microstrip antenna. Advanced Composites and Hybrid Materials, 2022, 5, 872-883.	21.1	32
143	Connectivity of organic matter pores in the Lower Silurian Longmaxi Formation shale, Sichuan Basin, Southern China: Analyses from helium ion microscope and focused ion beam scanning electron microscope. Geological Journal, 2022, 57, 1912-1924.	1.3	32
144	Distinct Temperature-Dependent CO ₂ Sorption of Two Isomeric Metal–Organic Frameworks. Crystal Growth and Design, 2014, 14, 2003-2008.	3.0	31

#	Article	IF	CITATIONS
145	Two Robust In(III)-Based Metal–Organic Frameworks with Higher Gas Separation, Efficient Carbon Dioxide Conversion, and Rapid Detection of Antibiotics. Inorganic Chemistry, 2020, 59, 5231-5239.	4.0	31
146	Microwave and traditional solvothermal syntheses, crystal structures, mass spectrometry and magnetic properties of Coll4O4 cubes. Dalton Transactions, 2013, 42, 5439.	3.3	30
147	A stable 3D porous coordination polymer as multi-chemosensor to Cr(<scp>iv</scp>) anion and Fe(<scp>iii</scp>) cation and its selective adsorption of malachite green oxalate dye. RSC Advances, 2015, 5, 97127-97132.	3.6	30
148	Catalytic Enantioselective Tautomerization of Metastable Enamines. Organic Letters, 2018, 20, 244-247.	4.6	30
149	A polar tetrazolyl-carboxyl microporous Zn(ii)–MOF: sorption and luminescent properties. Dalton Transactions, 2013, 42, 3653.	3.3	29
150	Four new 3D metal–organic frameworks constructed by the asymmetrical pentacarboxylate: gas sorption behaviour and magnetic properties. Dalton Transactions, 2016, 45, 15473-15480.	3.3	29
151	Effective C ₂ H ₂ Separation and Nitrofurazone Detection in a Stable Indium–Organic Framework. Inorganic Chemistry, 2020, 59, 2853-2860.	4.0	29
152	Fluorine-Substituted Regulation in Two Comparable Isostructural Cd(II) Coordination Polymers: Enhanced Fluorescence Detection for Tetracyclines in Water. Crystal Growth and Design, 2021, 21, 2488-2497.	3.0	29
153	Microporous Cd(II) Metal–Organic Framework for CO ₂ Catalysis, Luminescent Sensing, and Absorption of Methyl Green. Crystal Growth and Design, 2021, 21, 2734-2743.	3.0	29
154	Low-Pressure Selectivity, Stepwise Gas Sorption Behaviors, and Luminescent Properties (Experimental) Tj ETQqO Growth and Design, 2017, 17, 3965-3973.	0 0 rgBT / 3.0	Overlock 10 29
155	Amide-Functionalized In-MOF for Effective Hydrocarbon Separation and CO ₂ Catalytic Fixation. Inorganic Chemistry, 2022, 61, 2679-2685.	4.0	29
156	Generation of a sub-diffraction hollow ring by shaping an azimuthally polarized wave. Scientific Reports, 2016, 6, 37776.	3.3	28
157	A chiral metal–organic framework with polar channels: unique interweaving six-fold helices and high CO ₂ /CH ₄ separation. Inorganic Chemistry Frontiers, 2016, 3, 1326-1331.	6.0	28
158	Homo―and Heteroligand Polyâ€NHC Metal Assemblies: Synthesis by Narcissistic and Social Selfâ€Sorting. Angewandte Chemie, 2018, 130, 15993-15997.	2.0	28
159	A Dy ₆ -cluster-based <i>fcu</i> -MOF with efficient separation of C ₂ H ₂ /C ₂ H ₄ and selective adsorption of benzene. Inorganic Chemistry Frontiers, 2021, 8, 376-382.	6.0	28
160	An Efficient Strategy for Reinforcing Flexible Ceramic Membranes. Nano Letters, 2021, 21, 9419-9425.	9.1	28
161	Co-culture of endothelial cells and patterned smooth muscle cells on titanium: Construction with high density of endothelial cells and low density of smooth muscle cells. Biochemical and Biophysical Research Communications, 2015, 456, 555-561.	2.1	27
162	A Two-Coordinate Neutral Germylene Supported by a \hat{I}^2 -Diketiminate Ligand in the Radical State. Organometallics, 2017, 36, 2706-2709.	2.3	27

#	Article	IF	CITATIONS
163	UV-blocking, transparent and hazy cellulose nanopaper with superior strength based on varied components of poplar mechanical pulp. Cellulose, 2020, 27, 6563-6576.	4.9	27
164	Selective CO ₂ adsorption in a microporous metal–organic framework with suitable pore sizes and open metal sites. Inorganic Chemistry Frontiers, 2015, 2, 550-557.	6.0	26
165	Investigation of enhanced hemocompatibility and tissue compatibility associated with multi-functional coating based on hyaluronic acid and Type IV collagen. International Journal of Energy Production and Management, 2016, 3, 149-157.	3.7	26
166	Acetylene Separation by a Ca-MOF Containing Accessible Sites of Open Metal Centers and Organic Groups. ACS Applied Materials & amp; Interfaces, 2021, 13, 58862-58870.	8.0	26
167	Two New (3,6)-Connected Frameworks Based on an Unsymmetrical Tritopic Pyridyldicarboxylate Ligand and Co ₂ Dimer: Structures, Magnetic, and Sorption Properties. Crystal Growth and Design, 2013, 13, 701-707.	3.0	25
168	New two-dimensional Mn(ii) metal–organic framework featured spin canting. Dalton Transactions, 2013, 42, 7092.	3.3	25
169	Copper-Catalyzed Aerobic Oxidative Cyclization of Ketoxime Acetates with Pyridines for the Synthesis of Imidazo[1,2-a]pyridines. Synthesis, 2016, 48, 1920-1926.	2.3	25
170	Nickel-catalyzed carbonylation of arylboronic acids with DMF as a CO source. Organic Chemistry Frontiers, 2017, 4, 569-572.	4.5	25
171	An Interpenetrated Pillar-Layered Metal-Organic Framework with Novel Clusters: Reversible Structural Transformation and Selective Gate-Opening Adsorption. Crystal Growth and Design, 2018, 18, 3044-3050.	3.0	25
172	Design of Antiâ€UV Radiation Textiles with Selfâ€Assembled Metal–Organic Framework Coating. Advanced Materials Interfaces, 2020, 7, 1901525.	3.7	25
173	Design and preparation of new luminescent metal–organic frameworks and different doped isomers: sensing pollution ions and enhancement of gas capture capacity. Inorganic Chemistry Frontiers, 2021, 8, 286-295.	6.0	25
174	A 2-Fold Interpenetrated Nitrogen-Rich Metal–Organic Framework: Dye Adsorption and CO ₂ Capture and Conversion. Inorganic Chemistry, 2021, 60, 3156-3164.	4.0	25
175	Transparent and Hazy Eu _{<i>x</i>} Tb _{1–<i>x</i>} -Nanopaper with Color-Tuning, Photo-Switching, and White Light-Emitting Properties for Anti-counterfeiting and Light-Softened WLEDs. ACS Sustainable Chemistry and Engineering, 2021, 9, 5827-5837.	6.7	25
176	Dynamic porous coordination polymer based on 2D stacked layers exhibiting high sorption selectivity for CO2. Dalton Transactions, 2012, 41, 3209.	3.3	24
177	Iterative Mass Spectrometry and X-Ray Crystallography to Study Ion-Trapping and Rearrangements by a Flexible Cluster. Scientific Reports, 2013, 3, 3516.	3.3	24
178	Thermally Triggered Solidâ€State Singleâ€Crystalâ€toâ€Singleâ€Crystal Structural Transformation Accompanies Property Changes. Chemistry - A European Journal, 2015, 21, 4703-4711.	3.3	24
179	Constructing bio-functional layers of hyaluronan and type IV collagen on titanium surface for improving endothelialization. Journal of Materials Science, 2015, 50, 3226-3236.	3.7	24
180	Design, synthesis, insecticidal activity and 3D-QSR study for novel trifluoromethyl pyridine derivatives containing an 1,3,4-oxadiazole moiety. RSC Advances, 2018, 8, 6306-6314.	3.6	24

#	Article	IF	CITATIONS
181	An NIF-doped ZIF-8 hybrid membrane for continuous antimicrobial treatment. RSC Advances, 2020, 10, 7360-7367.	3.6	24
182	Metal–Organic Frameworks as Heterogeneous Electrocatalysts for Water Splitting and CO ₂ Fixation. Crystal Growth and Design, 2021, 21, 3123-3142.	3.0	24
183	Construction of Highly Porous Pillared Metal–Organic Frameworks: Rational Synthesis, Structure, and Gas Sorption Properties. Inorganic Chemistry, 2017, 56, 9147-9155.	4.0	23
184	Planar binary-phase lens for super-oscillatory optical hollow needles. Scientific Reports, 2017, 7, 4697.	3.3	23
185	Four alkaline earth metal (Mg, Ca, Sr, Ba)-based MOFs as multiresponsive fluorescent sensors for Fe3+, Pb2+ and Cu2+ ions in aqueous solution. Journal of Solid State Chemistry, 2019, 277, 636-647.	2.9	23
186	Mutations in TOMM70 lead to multi-OXPHOS deficiencies and cause severe anemia, lactic acidosis, and developmental delay. Journal of Human Genetics, 2020, 65, 231-240.	2.3	23
187	A Facile Reaction Strategy for the Synthesis of MOF-Based Pine-Needle-Like Nanocluster Hierarchical Structure for Efficient Overall Water Splitting. Inorganic Chemistry, 2021, 60, 4047-4057.	4.0	23
188	Efficient Gas and VOC Separation and Pesticide Detection in a Highly Stable Interpenetrated Indium–Organic Framework. Inorganic Chemistry, 2021, 60, 10698-10706.	4.0	23
189	Lanthanide–Organic Frameworks with Uncoordinated Lewis Base Sites: Tunable Luminescence, Antibiotic Detection, and Anticounterfeiting. Inorganic Chemistry, 2022, 61, 6101-6109.	4.0	23
190	Ligand Configuration-Induced Manganese(II) Coordination Polymers: Syntheses, Crystal Structures, Sorption, and Magnetic Properties. Inorganic Chemistry, 2017, 56, 10090-10098.	4.0	22
191	A Flexible and Stable Interpenetrated Indium Pyridylcarboxylate Framework with Breathing Behaviors and Highly Selective Adsorption of Cationic Dyes. Inorganic Chemistry, 2019, 58, 4019-4025.	4.0	22
192	Holographic Super-Resolution Metalens for Achromatic Sub-Wavelength Focusing. ACS Photonics, 2021, 8, 2294-2303.	6.6	22
193	Mutations in <i>FASTKD2</i> are associated with mitochondrial disease with multiâ€OXPHOS deficiency. Human Mutation, 2020, 41, 961-972.	2.5	21
194	Highly flexible ceramic nanofibrous membranes for superior thermal insulation and fire retardancy. Nano Research, 2022, 15, 2592-2598.	10.4	21
195	Copper-catalyzed carbonylation of anilines by diisopropyl azodicarboxylate for the synthesis of carbamates. RSC Advances, 2016, 6, 107542-107546.	3.6	20
196	K ₂ CO ₃ -Mediated Cyclization and Rearrangement of î³,î´-Alkynyl Oximes To Form Pyridols. Organic Letters, 2017, 19, 1574-1577.	4.6	20
197	A new layer-stacked porous framework showing sorption selectivity for CO ₂ and luminescence. Dalton Transactions, 2017, 46, 11722-11727.	3.3	20
198	Cellulose nanopaper with controllable optical haze and high efficiency ultraviolet blocking for flexible optoelectronics. Cellulose, 2019, 26, 2201-2208.	4.9	20

#	Article	IF	CITATIONS
199	Supramolecular-induced regiocontrol over the photochemical [4 + 4] cyclodimerization of NHC- or azole-substituted anthracenes. Chemical Science, 2021, 12, 2165-2171.	7.4	20
200	Fine-Tuning the Porosities of the Entangled Isostructural Zn(II)-Based Metal–Organic Frameworks with Active Sites by Introducing Different N-Auxiliary Ligands: Selective Gas Sorption and Efficient CO ₂ Conversion. Inorganic Chemistry, 2020, 59, 2450-2457.	4.0	20
201	Reaction-determined assemblies of 0D to 3D complexes: structural diversities and luminescence properties. CrystEngComm, 2016, 18, 3358-3371.	2.6	19
202	Two {Dy ₂ } single-molecule magnets formed via an in situ reaction by capturing CO ₂ from atmosphere under ambient conditions. Dalton Transactions, 2017, 46, 1753-1756.	3.3	19
203	PhI(OAc)2-promoted umpolung acetoxylation of enamides for the synthesis of α-acetoxy ketones. Science China Chemistry, 2017, 60, 761-768.	8.2	19
204	Two metal–organic frameworks based on a flexible benzimidazole carboxylic acid ligand: selective gas sorption and luminescence. Dalton Transactions, 2017, 46, 15118-15123.	3.3	19
205	Comparative Study on Temperature-Dependent CO ₂ Sorption Behaviors of Two Isostructural <i>N</i> -Oxide-Functionalized 3D Dynamic Microporous MOFs. Inorganic Chemistry, 2018, 57, 1455-1463.	4.0	19
206	Luminescence sensing and supercapacitor performances of a new (3,3)-connected Cd-MOF . CrystEngComm, 2019, 21, 6186-6195.	2.6	19
207	Rational synthesis of an ultra-stable Zn(<scp>ii</scp>) coordination polymer based on a new tripodal pyrazole ligand for the highly sensitive and selective detection of Fe ³⁺ and Cr ₂ O ₇ ^{2â°} in aqueous media. Dalton Transactions, 2020, 49, 11201-11208.	3.3	19
208	Zeolitic Metal Cluster Carboxylic Framework for Selective Carbon Dioxide Chemical Fixation through the Superlarge Cage. Inorganic Chemistry, 2020, 59, 3912-3918.	4.0	19
209	Determination of cyflufenamid residues in 12 foodstuffs by QuEChERS-HPLC-MS/MS. Food Chemistry, 2021, 362, 130148.	8.2	19
210	Base-mediated formal [3+2] cycloaddition of β,γ-alkenyl esters and p-TsN3 for the synthesis of pyrazoles. Science Bulletin, 2017, 62, 493-496.	9.0	18
211	Irreversible Solvatochromic Zn-Nanopaper Based on Zn(II) Terpyridine Assembly and Oxidized Nanofibrillated Cellulose. ACS Sustainable Chemistry and Engineering, 2018, 6, 11614-11623.	6.7	18
212	Three New MOFs Induced by Organic Linker Coordination Modes: Gas Sorption, Luminescence, and Magnetic Properties. Chemistry - an Asian Journal, 2019, 14, 2988-2994.	3.3	18
213	Tetranuclear dysprosium single-molecule magnets: tunable magnetic interactions and magnetization dynamics through modifying coordination number. Dalton Transactions, 2019, 48, 2135-2141.	3.3	18
214	Dramatic impact of auxiliary ligands on the two-step magnetic relaxation process in Dy ₄ (<scp>iii</scp>) single-molecule magnets. Dalton Transactions, 2019, 48, 5793-5799.	3.3	18
215	Water soluble Ln(III)-based metallopolymer with AIE-active and ACQ-effect lanthanide behaviors for detection of nanomolar pyrophosphate. Sensors and Actuators B: Chemical, 2019, 282, 999-1007.	7.8	18
216	Three Lanthanide Metalâ€Organic Frameworks Based on an Etherâ€Decorated Polycarboxylic Acid Linker: Luminescence Modulation, CO ₂ Capture and Conversion Properties. Chemistry - an Asian Journal, 2020, 15, 191-197.	3.3	18

#	Article	IF	CITATIONS
217	Rational Stepwise Construction of Different Heterometallic–Organic Frameworks (HMOFs) for Highly Efficient CO ₂ Conversion. Chemistry - A European Journal, 2020, 26, 5400-5406.	3.3	18
218	A new porous Co(<scp>ii</scp>)-metal–organic framework for high sorption selectivity and affinity to CO ₂ and efficient catalytic oxidation of benzyl alcohols to benzaldehydes. CrystEngComm, 2021, 23, 3717-3723.	2.6	18
219	Discussion about initial runoff and volume capture ratio of annual rainfall. Water Science and Technology, 2016, 74, 1764-1772.	2.5	17
220	C ₃ ‣ymmetric Assemblies from Trigonal Polycarbene Ligands and M ^I lons for the Synthesis of Threeâ€Ðimensional Polyimidazolium Cations. Angewandte Chemie, 2019, 131, 13494-13498.	2.0	17
221	Synthesis, Characterization, and Properties of Organometallic Molecular Cylinders Bearing Bulky Imidazo[1,5â€ <i>a</i>]pyridineâ€Based Nâ€Heterocyclic Carbene Ligands. Chemistry - A European Journal, 2019, 25, 5472-5479.	3.3	17
222	Five new 3D transition MOFs based on 1-(3,5-dicarboxylatobenzyl)-3,5-pyrazole dicarboxylic acid displaying unique luminescence sensing towards Fe ³⁺ and magnetic properties. Dalton Transactions, 2019, 48, 7786-7793.	3.3	17
223	Highly Thermally and Chemically Stable Nickel(II) Coordination Polymers: Tentative Studies on Their Sorption, Catalysis, and Magnetism. Crystal Growth and Design, 2019, 19, 797-807.	3.0	17
224	Aggregation-induced white emission of lanthanide metallopolymer and its coating on cellulose nanopaper for white-light softening. Journal of Materials Chemistry C, 2020, 8, 2205-2210.	5.5	17
225	Stable Indium Pyridylcarboxylate Framework with Highly Selective Adsorption of Cationic Dyes and Effective Nitenpyram Detection. Inorganic Chemistry, 2021, 60, 5232-5239.	4.0	17
226	C ₂ H ₂ capture and separation in a MOF based on Ni ₆ trigonal-prismatic units. Chemical Communications, 2022, 58, 6208-6211.	4.1	17
227	Determination of dopamine using the fluorescence quenching of 2, 3-diaminophenazine. Instrumentation Science and Technology, 2017, 45, 101-110.	1.8	16
228	On/off fluorescence emission induced by encapsulation, exchange and reversible encapsulation of a BODIPY-guest in self-assembled organometallic cages. Dalton Transactions, 2019, 48, 7236-7241.	3.3	16
229	The effect of coordinated solvent molecules on metal coordination environments in single-crystal-to-single-crystal transformations. CrystEngComm, 2020, 22, 6750-6775.	2.6	16
230	A stable Cd(II)-based MOF with efficient CO2 capture and conversion, and fluorescence sensing for ronidazole and dimetridazole. Journal of Solid State Chemistry, 2021, 295, 121890.	2.9	16
231	Efficient One-Step Purification of C ₁ and C ₂ Hydrocarbons over CO ₂ in a New CO ₂ -Selective MOF with a Gate-Opening Effect. ACS Applied Materials & Interfaces, 2022, 14, 26858-26865.	8.0	16
232	Two Comparable Isostructural Microporous Metal-Organic Frameworks: Better Luminescent Sensor and Higher Adsorption Selectivity for the Fluorine-Decorated Framework. European Journal of Inorganic Chemistry, 2015, 2015, 5773-5780.	2.0	15
233	Luminescence Sensing of Fe ³⁺ and Nitrobenzene by Three Isostructural Ln–MOFs Assembled by a Phenylâ€Đicarboxylate Ligand. ChemistrySelect, 2019, 4, 12794-12800.	1.5	15
234	Constructions of new luminescent 3D porous MOFs with high stability, unique selectivity and low detection limits for various ions in aqueous solution. Journal of Solid State Chemistry, 2020, 285, 121270.	2.9	15

#	Article	IF	CITATIONS
235	One‣tep C ₂ H ₄ Purification from Ternary C ₂ H ₆ /C ₂ /C <sub>/C<sub>/C₂H₂/C<sub>/C₂/C<sub>/C₂/C<sub>/C<sub>/C₂/C<sub>/C<sub>/C<sub>/C<sub>/C<sub>/C<sub>/C<sub>/C<sub>/C<sub>/C<sub>/C<sub>/C<sub>/C<sub>/C<sub>/C<sub>/C<sub>/C<sub>/C<sub>/C<sub>/C<sub>/C<sub>/C<sub>/C<sub>/C<sub>/C<sub>/C<sub>/C<sub>/C<sub>/C<sub>/C<sub>/C<sub>/C<sub>/C<sub>/C<sub>/C<sub>/C<sub>/C<sub>/C<sub>/C<sub>/C<sub>/C<sub>/C<sub>/C<sub>/C<sub>/C<sub>/C<sub>/C<sub>/C<sub>/C<sub>/C<sub>/C<sub>/C<sub>/C<sub>/C<sub>/C<sub>/C<sub>/C<sub>/C<sub>/C<sub>/C<sub>/C<sub>/C<sub>/C<sub>/C<sub>/C<sub>/C<sub>/C<sub>/C<sub>/C<sub>/C<sub>/C<sub>/C<sub>/C<sub>/C<sub>/C<sub>/C<sub>/C<sub c<su<="" c_{<td>2.0</td><td>15</td>}</sub></sub></sub></sub></sub></sub></sub></sub></sub></sub></sub></sub></sub></sub></sub></sub></sub></sub></sub></sub></sub></sub></sub></sub></sub></sub></sub></sub></sub></sub></sub></sub></sub></sub></sub></sub></sub></sub></sub></sub></sub></sub></sub></sub></sub></sub></sub></sub></sub></sub></sub></sub></sub></sub></sub></sub></sub></sub></sub></sub></sub></sub></sub></sub></sub></sub></sub></sub></sub></sub></sub></sub></sub></sub></sub></sub></sub></sub></sub></sub></sub></sub>	2.0	15
236	Peculiar phenomena of structural transformations triggered from a nickel coordination polymer. CrystEngComm, 2015, 17, 1839-1847.	2.6	14
237	Reaction-controlled assemblies and structural diversities of seven Co(<scp>ii</scp>)/Cu(<scp>ii</scp>) complexes based on a bipyridine-dicarboxylate N-oxide ligand. CrystEngComm, 2015, 17, 775-786.	2.6	14
238	Five 1D to 3D Zn(<scp>ii</scp>)/Mn(<scp>ii</scp>)-CPs based on dicarboxyphenyl-terpyridine ligand: stepwise adsorptivity and magnetic properties. CrystEngComm, 2017, 19, 4789-4796.	2.6	14
239	New Supercage Metal–Organic Framework Based on Allopurinol Ligands Showing Acetylene Storage and Separation. Chemistry - A European Journal, 2020, 26, 16402-16407.	3.3	14
240	Size Effect of Arylenediimide π-Conjugate Systems on the Photoresponsive Behaviors in Eu ³⁺ -Based Coordination Polymers. Inorganic Chemistry, 2022, 61, 6403-6410.	4.0	14
241	Comparative Study of Structures and Luminescent Properties of Three Ag(I) Complexes Utilizing an Achiral Bipyridyl- <i>N</i> or Its Axially Chiral <i>N</i> -Oxide Analogue. Crystal Growth and Design, 2018, 18, 2784-2794.	3.0	13
242	Sonodynamic therapy induces oxidative stress, DNA damage and apoptosis in glioma cells. RSC Advances, 2018, 8, 36245-36256.	3.6	13
243	Luminescent and Magnetic Properties of Coordination Polymers Induced by Coordinating Modes of a Bis(oxamate) Ligand. ChemPlusChem, 2019, 84, 62-68.	2.8	13
244	Luminescence tuning and sensing properties of stable 2D lanthanide metal–organic frameworks built with symmetrical flexible tricarboxylic acid ligands containing ether oxygen bonds. CrystEngComm, 2021, 23, 411-418.	2.6	13
245	Electrochemical Performance of Coaxially Wet-Spun Hierarchically Porous Lignin-Based Carbon/Graphene Fiber Electrodes for Flexible Supercapacitors. ACS Applied Energy Materials, 2021, 4, 9077-9089.	5.1	13
246	Ge ^I –Ge ^I Coupling Reaction Induced by a Mixture of CoBr ₂ and a Seven-Membered N-Heterocyclic Carbene. Inorganic Chemistry, 2018, 57, 2969-2972.	4.0	12
247	A dinuclear dysprosium single-molecule magnet constructed by o-vanillin Schiff base ligand: Magnetic properties and solution behaviour. Inorganic Chemistry Communication, 2017, 76, 103-107.	3.9	11
248	The influence of coordination modes and active sites of a 5-(triazol-1-yl) nicotinic ligand on the assembly of diverse MOFs. Dalton Transactions, 2017, 46, 9784-9793.	3.3	11
249	Five complexes based on a new racemic tetraoxaspiro ligand: correlation of potential coordination preferences with the structure, magnetic properties and luminescence properties. Dalton Transactions, 2019, 48, 3862-3873.	3.3	11
250	Supramolecular Construction of a [16]â€lmidazolium Cage via a Quadruple [2+2] Photocycloaddition and Its Selective Fluorescent Recognition of Pyranine (HPTS). Chemistry - A European Journal, 2020, 26, 7190-7193.	3.3	11
251	Regulation mechanism of graphene oxide on the structure and mechanical properties of bio-based gel-spun lignin/poly (vinyl alcohol) fibers. Cellulose, 2021, 28, 4745-4760.	4.9	11
252	Significant centre metallic effects on the sensing properties of two isostructural lanthanide metal-organic frameworks. Inorganic Chemistry Communication, 2017, 79, 12-16.	3.9	10

#	Article	IF	CITATIONS
253	Palladium-catalyzed oxidative carbonylation of N-aryl enamino esters with CO and alcohols: synthesis of N-aryl aminomethylenemalonates. Chemical Communications, 2017, 53, 6243-6246.	4.1	10
254	Three new super water-stable lanthanide–organic frameworks for luminescence sensing and magnetic properties. New Journal of Chemistry, 2018, 42, 9221-9227.	2.8	10
255	Range-Broadening Ultraviolet-Blocking Regulation of Cellulose Nanopaper via Surface Self-Absorption with Poly(methyl methacrylate)/Avobenzone. ACS Applied Polymer Materials, 2019, 1, 2981-2989.	4.4	10
256	Four new water-stable metal-organic frameworks based on diverse metal clusters: Syntheses, structures, and luminescent sensing properties. Journal of Solid State Chemistry, 2019, 269, 386-395.	2.9	10
257	Effect of organic grafting expandable graphite on combustion behaviors and thermal stability of lowâ€density polyethylene composites. Polymer Composites, 2020, 41, 719-728.	4.6	10
258	Four new metal-organic frameworks based on diverse metal clusters: Syntheses, structures, luminescent sensing and dye adsorption properties. Journal of Solid State Chemistry, 2020, 287, 121336.	2.9	10
259	Effect of latter feeding wire on double-wire GTA-AM stainless steel. Materials and Manufacturing Processes, 2021, 36, 608-617.	4.7	10
260	A scalable strategy toward compliant tandem yarn-shaped supercapacitors with high voltage output. Journal of Materials Chemistry A, 2021, 9, 13916-13925.	10.3	10
261	Assessment of mitochondrial function in metabolic dysfunction-associated fatty liver disease using obese mouse models. Zoological Research, 2020, 41, 539-551.	2.1	10
262	A new metal–organic framework based on rare [Zn ₄ F ₄] cores for efficient separation of C ₂ H ₂ . Chemical Communications, 2021, 57, 12788-12791.	4.1	10
263	Highly Efficient I ₂ Sorption, CO ₂ Capture, and Catalytic Conversion by Introducing Nitrogen Donor Sites in a Microporous Co(II)-Based Metal–Organic Framework. Inorganic Chemistry, 2022, 61, 7005-7016.	4.0	10
264	Evaluation of Faecalibacterium 16S rDNA genetic markers for accurate identification of swine faecal waste by quantitative PCR. Journal of Environmental Management, 2016, 181, 193-200.	7.8	9
265	Two isostructural Ln-MOFs showing luminescent sensing (Eu) and slow magnetic relaxation (Dy) properties. Dalton Transactions, 2018, 47, 15656-15660.	3.3	9
266	New porous Co(II)-based metal-organic framework including 1D ferromagnetic chains with highly selective gas adsorption and slow magnetic relaxation. Journal of Solid State Chemistry, 2019, 276, 226-231.	2.9	9
267	A Tetra-amido-Protected Ge ₅ -Spiropentadiene. Journal of the American Chemical Society, 2019, 141, 19252-19256.	13.7	9
268	Synergistic effects of red phosphorus masterbatch with expandable graphite on the flammability and thermal stability of polypropylene/thermoplastic polyurethane blends. Polymers and Polymer Composites, 2020, 28, 209-219.	1.9	9
269	A copper-catalyzed reaction of oximes with diisopropyl azodicarboxylate: an alternative method for the synthesis of oxime carbonates. Organic and Biomolecular Chemistry, 2017, 15, 1091-1095.	2.8	8
270	Solvent-induced diversity of luminescent metal–organic frameworks based on different secondary building units. RSC Advances, 2017, 7, 46125-46131.	3.6	8

#	Article	IF	CITATIONS
271	Seven new complexes based on various coordination modes of bifunctional ligand: Luminescent sensing and magnetic properties. Inorganica Chimica Acta, 2019, 495, 118971.	2.4	8
272	Two new MOFs based on 5-((4-carboxypyridin-2-yl)oxy) isophthalic acid displaying unique selective CO ₂ gas adsorption and magnetic properties. CrystEngComm, 2019, 21, 7078-7084.	2.6	8
273	Process-tracing study on the post-assembly modification of poly-NHC-based metallosupramolecular cylinders with tunable aggregation-induced emission. Chemical Communications, 2019, 55, 13689-13692.	4.1	8
274	One-pot green synthesis of enamides and 1,3-diynes. Chinese Journal of Catalysis, 2015, 36, 113-118.	14.0	7
275	Neon ion beam induced pattern formation on amorphous carbon surfaces. AIP Advances, 2018, 8, .	1.3	7
276	Two alkaline earth metal coordination polymers based on a new oxamate-dicarboxylate ligand: Selective fluorescence sensing of Fe3+ in aqueous solution. Inorganic Chemistry Communication, 2019, 107, 107490.	3.9	7
277	Five new coordination polymers of s- and d-block metals: Structural diversities, magnetic properties and luminescence. Journal of Solid State Chemistry, 2019, 270, 516-523.	2.9	7
278	Pr and Mo Coâ€Doped SrFeO _{3–<i>δ</i>} as an Efficient Cathode for Pure CO ₂ Reduction Reaction in a Solid Oxide Electrolysis Cell. Energy Technology, 2020, 8, 2000539.	3.8	7
279	Momentary lapses of attention in multisensory environment. Cortex, 2020, 131, 195-209.	2.4	7
280	A Silylene–Germylene Molecule Containing a Si ^I â^'Ge ^I Single Bond. Chemistry - A European Journal, 2020, 26, 6122-6125.	3.3	7
281	Molecular characterization and functional expression of voltageâ€gated sodium channel variants in <i>Apolygus lucorum</i> (<scp>Meyerâ€DĂ¼r</scp>). Pest Management Science, 2020, 76, 2095-2104.	3.4	7
282	A multi-functional two-dimensional Zn(<scp>ii</scp>)-organic framework for selective carbon dioxide adsorption, sensing of nitrobenzene and Cr ₂ O ₇ ^{2â^'} . CrystEngComm, 2021, 23, 7643-7649.	2.6	7
283	Sieving Effect for the Separation of C ₂ H ₂ /C ₂ H ₄ in an Ultrastable Ultramicroporous Zincâ€Organic Framework. Chemistry - an Asian Journal, 2021, 16, 1233-1236.	3.3	7
284	Ultra-high adsorption selectivity and affinity for CO2 over CH4, and luminescent properties of three new solvents induced Zn(II)-based metal-organic frameworks (MOFs). Journal of Solid State Chemistry, 2021, 297, 122054.	2.9	7
285	Mechanical properties and microstructure of Al2O3/TiAl in situ composites doped with Cr and V2O5. Science of Sintering, 2012, 44, 73-80.	1.4	7
286	Fabrication of a series of isostructural water-stable lanthanide metal-organic frameworks: Tunable luminescence, sensing for antibiotics and magnetic properties. Journal of Solid State Chemistry, 2022, 309, 123003.	2.9	7
287	Improved performance of the pyrimidine-modified porous In-MOF and an <i>in situ</i> prepared composite Ag@In-MOF material. Chemical Communications, 2022, 58, 7749-7752.	4.1	7
288	The Microstructures and Mechanical Properties of V2O5-Doped Al2O3/TiAl In-Situ Composites by Reactive Hot Pressing Process. Journal of Materials Engineering and Performance, 2013, 22, 3933-3939.	2.5	6

#	Article	IF	CITATIONS
289	A Pb ²⁺ -based coordination polymer with 5-(1H-tetrazol-5-yl)isophthalic acid ligand: structure and photoluminescence. Journal of Coordination Chemistry, 2016, 69, 2573-2579.	2.2	6
290	Structural Diversity of Three Pyrazoyl–Carboxyl Bifunctional Ligandâ€Based Metal–Organic Frameworks: Luminescence and Magnetic Properties. ChemPlusChem, 2017, 82, 376-382.	2.8	6
291	Four New Stable Lanthanide Organic Frameworks: Highly Selective Luminescent Sensing and Magnetic Properties. ChemistrySelect, 2018, 3, 3214-3220.	1.5	6
292	Tetranuclear dysprosium compound: Synthesis and single-molecule magnet properties. Journal of Solid State Chemistry, 2019, 273, 11-16.	2.9	6
293	A new 3D luminescent Ba-organic framework with high open metal sites: CO ₂ fixation, luminescence sensing, and dye sorption. CrystEngComm, 2021, 23, 663-670.	2.6	6
294	An excellent thermostable dual-functionalized 3D <i>fsx</i> -type Cd(<scp>ii</scp>) MOF for the highly selective detection of Fe ³⁺ ions and ten nitroaromatic explosives. CrystEngComm, 2021, 23, 6171-6179.	2.6	6
295	Supramolecular Coordination Cages Based on Nâ€Heterocyclic Carbeneâ€Gold(I) Ligands and Their Precursors: Selfâ€Assembly, Structural Transformation and Guestâ€Binding Properties. Chemistry - A European Journal, 2021, 27, 7853-7861.	3.3	6
296	Two porous three-dimensional (3D) metal–organic frameworks based on diverse metal clusters: selective sensing of Fe ³⁺ and Cr ₂ O ₇ ^{2â^'} . New Journal of Chemistry, 2022, 46, 4292-4299.	2.8	6
297	Highly Enhanced Congo Red Sorption of New Functionalized Porous Eu(III)–Organic Framework by the Insertion of Sulfonate Groups. Crystal Growth and Design, 0, , .	3.0	6
298	A Lead Carboxylateâ€Azolate Metalâ€Organic Framework Based on Hexanuclear Clusters: Luminescence and Accelerating the Thermal Decomposition of Ammonium Perchlorate. ChemPlusChem, 2019, 84, 289-294.	2.8	5
299	The synergistic flame retardancy of modified expandable graphite and metal hydroxides on HDPE/EVA composites. Journal of Thermoplastic Composite Materials, 2022, 35, 782-798.	4.2	5
300	Luminescent metal-organic frameworks constructed by a V-shaped pentacarboxylic acid ligand as bifunctional chemosensors for Fe3+ and Cr2O72 Journal of Solid State Chemistry, 2022, 309, 122988.	2.9	5
301	Dyestuff wastewater treatment by combined SDS-CuO/TiO2 photocatalysis and sequencing batch reactor. Journal of Central South University, 2012, 19, 1685-1692.	3.0	4
302	Six Coordination Polymers based on 4â€(1Hâ€Imidazolâ€1â€yl)phthalic Acid: Structural Diversities, Magnetism and Luminescence Properties. Zeitschrift Fur Anorganische Und Allgemeine Chemie, 2018, 644, 504-511.	1.2	4
303	Investigation into surface composition of nitrogen-doped niobium for superconducting RF cavities. Nanotechnology, 2021, 32, 245701.	2.6	4
304	Efficient Asymmetric Biomimetic Aldol Reaction of Glycinates and Trifluoromethyl Ketones by Carbonyl Catalysis. Angewandte Chemie, 2021, 133, 20328-20334.	2.0	4
305	Fe-doped CoFe–P phosphides nanosheets dispersed on nickel foam derived from Prussian blue analogues as efficient electrocatalysts for the oxygen evolution reaction. Journal of Solid State Chemistry, 2022, 311, 123084.	2.9	4
306	Phase-mediated controllable intramolecular and intermolecular photocycloadditions assisted by supramolecular templates. Science China Chemistry, 2022, 65, 1129-1133.	8.2	4

#	Article	IF	CITATIONS
307	Effect of Mn content on the microstructure and mechanical properties of (Ti,Mn)Al/Al ₂ O ₃ in situ composites prepared by hot pressing. Journal of Materials Research, 2013, 28, 1574-1581.	2.6	3
308	Two classic mutations in the linkerâ€helix <scp>IIL45</scp> and segment <scp>IIS6</scp> of <i>Apolygus lucorum</i> sodium channel confer pyrethroid resistance. Pest Management Science, 2020, 76, 3954-3964.	3.4	3
309	Alloying Cr2/3Te in AgCrSe2 compound for improving thermoelectrics. Applied Physics Letters, 2021, 118, 193902.	3.3	3
310	A new multi-functional Cu(<scp>ii</scp>)-organic framework as a platform for selective carbon dioxide chemical fixation and separation of organic dyes. CrystEngComm, 2021, 23, 8315-8322.	2.6	3
311	A microporous anionic metal–organic framework for aqueous encapsulation and highly reversible sensitization of light-emitting Tb ³⁺ ions. New Journal of Chemistry, 2022, 46, 5201-5205.	2.8	3
312	N-doped carbon material encapsulated cobalt nanoparticles for bifunctional electrocatalysts derived from a porous Co(II)-based metal-organic frameworks (MOFs). Journal of Solid State Chemistry, 2022, 309, 122989.	2.9	3
313	Study on Reasonable Chain Pillar Size in a Thick Coal Seam. Geofluids, 2022, 2022, 1-14.	0.7	3
314	Effects of distribution and growth orientation of precipitates on oxidation resistance of Cu–Cu ₁₂ –[Cr _{<i>x</i>/(12+<i>x</i>)} Ni _{12/(12+<i>x</i>)}] alloys. Journal of Materials Research, 2015, 30, 3299-3306.	>2.6	2
315	Study of Corrosion Behaviors of 316L Stainless Steel Welds in Liquid Lithium with Hydrogen Impurity. Fusion Science and Technology, 2019, 75, 104-111.	1.1	2
316	Two Cu-based cluster coordination polymers constructed from two thioether tripod tricarboxylic acid ligands: Synthesis, crystal structure and fluorescence sensing. Inorganic Chemistry Communication, 2020, 113, 107805.	3.9	2
317	A novel switch beam design method with extending switching radio-frequency bandwidth. Microsystem Technologies, 2021, 27, 315-324.	2.0	2
318	Systematic and efficient synthesis of β-diketiminato aluminum halides and their structural characterization. Tetrahedron Letters, 2021, 68, 152942.	1.4	2
319	Two novel luminescent metal-organic frameworks based on the thioether bond modification: The selective sensing and effective CO2 fixation. Journal of Solid State Chemistry, 2022, 307, 122813.	2.9	2
320	Design and Synthesis of Four Newly Water-Stable Pb-Based Heterometallic Organic Frameworks: How Do the Second Metals (Zn, Cd, Co, and Mn) Optimize Their Fluorescent and Catalytic Properties?. Crystal Growth and Design, 2022, 22, 2628-2636.	3.0	2
321	Comparison and Conversion of Dynamic Models of Speed Governor for Transient Stability Analysis in BPA and PSS/E. , 2010, , .		1
322	Equivalent model optimization with cyclic correction approximation method considering parasitic effect for thermoelectric coolers. Scientific Reports, 2017, 7, 15917.	3.3	1
323	Substituent changes in the salen ligands of CullNal-complexes to induce various structures and catalytic activities towards 2-imidazolines from nitriles and 1,2-diaminopropane. Chemical Communications, 2019, 55, 4619-4622.	4.1	1
324	Uncommon thioether-modified metal–organic frameworks with unique selective CO ₂ sorption and efficient catalytic conversion. CrystEngComm, 2021, 23, 1447-1454.	2.6	1

#	Article	IF	CITATIONS
325	Investigation of the Oxidation Behavior of Cr20Mn17Fe18Ta23W22 and Microdefects Evolution Induced by Hydrogen Ions before and after Oxidation. Materials, 2022, 15, 1895.	2.9	1
326	Evaluation of the site-unspecified peptide identification method for proteolytic peptide mapping. RSC Advances, 2020, 10, 37182-37186.	3.6	0
327	Frontispiz: Efficient Asymmetric Biomimetic Aldol Reaction of Glycinates and Trifluoromethyl Ketones by Carbonyl Catalysis. Angewandte Chemie, 2021, 133, .	2.0	0
328	Frontispiece: Efficient Asymmetric Biomimetic Aldol Reaction of Glycinates and Trifluoromethyl Ketones by Carbonyl Catalysis. Angewandte Chemie - International Edition, 2021, 60, .	13.8	0
329	Influence of Organic Matter on Gas-Bearing Properties and Analysis of Sedimentary Mechanism of Organic Matter Enrichment: A Case Study on the Yangtze Region of Southern China during the Early Cambrian. Geofluids, 2022, 2022, 1-12.	0.7	0